

Near Infrared Diode Laser Based Spectroscopic Detection of Ammonia: A Comparative Study of Photoacoustic and Direct Optical Absorption Methods

Zoltán Bozóki

Research Group on Laser Physics of the Hungarian Academy of Sciences, H-6701 Pf. 406 Szeged, HUNGARY

Árpád Mohácsi, Gábor Szabó and Zsolt Bor

Department of Optics and Quantum Electronics, University of Szeged, H-6701 Pf. 406 Szeged, HUNGARY

Miklós Erdélyi, Weidong Chen and Frank K. Tittel

Rice Quantum Institute, Rice University, Houston, TX 77005, USA

Abstract: A photoacoustic spectroscopic (PAS) and a direct optical absorption spectroscopic (OAS) gas sensor, both using continuous wave, room temperature diode lasers operating at 1531.8 nm, were compared on the basis of ammonia detection. Excellent linear correlation between the detector signals of the two systems was found. Although the physical properties and the mode of operation of both sensors were significantly different, their performances were found to be remarkably similar, with sub-ppm level minimum detectable concentration of ammonia and a fast response time in the range of a few minutes.

Index Heading: Photoacoustic Spectroscopy, Laser Absorption Spectroscopy, Gas Detection, Diode Lasers

1. Introduction

The motivation for ammonia concentration measurements at ppm, or sub-ppm levels includes applications such as the monitoring of thermal deNO_x processes¹, process control in semiconductor manufacturing², environmental monitoring³ and medical diagnostics⁴. Recent availability of near infrared (1.3 to 2 μm) distributed feedback (*DFB*) diode lasers with relatively large continuous-wave (cw) powers, and narrow spectral line-widths, has led to the interest in gas sensors based on overtone and combination band absorption spectroscopy⁵. The application of these lasers is limited by their narrow tuning range. Analysis of multi-component mixtures requires the use of tunable laser sources such as external cavity diode lasers⁶. From the spectroscopic point of view, the sensitivity of diode laser based ammonia detection systems is due to the relatively strong overtone absorption band of the ammonia molecule in the near infrared, accessible with AlGaAs based room temperature telecommunication type diode lasers^{5,7}. The highly asymmetric N-H bond of the ammonia molecule results in a high-energy, fundamental transition together with a high transition probability for overtones. Hence, ammonia absorption lines with line strength of $\sim 10^{-21}$ cm/molecule are accessible in the 1.53 μm wavelength range⁸. Due to similar spectroscopic properties, other molecules with X-H bond, such as water vapor and methane can also be detected with sub-ppm level sensitivity in the near infrared wavelength range^{9,10}.

The merits of both optical absorption spectroscopic (*OAS*) and photoacoustic spectroscopic (*PAS*) detection for various gas concentration measurement applications have been described in Ref. 11. Both techniques were already applied successfully for ammonia detection^{12,13}.

A direct comparison of *OAS* and *PAS* detection methods applied to methane concentration measurements was reported by Schäfer *et. al.*¹⁴. They found that the *OAS* detection outperformed the *PAS* detection with demonstrated sensitivities of 1.15 ppm and 120

ppm, respectively. However, recently a significantly improved sensitivity of 3 ppm was reported for *PAS* detection of methane⁹. These previous studies provided valuable inputs to the comparison study of *PAS* and *OAS* sensors, reported in this work. First, the configurations of both sensors are described and their respective technical characteristics (with special emphasis on the two gas cells employed) are compared. This is followed by a discussion of the background signals, their sources and the extent to which they limit the analyzer performance. Finally, the modes of operation and performance characteristics of the two diode laser based spectroscopic systems are compared. Table 1 provides a convenient summary of the reported work.

2. Experimental comparison of the two gas sensor systems

The experimental setup shown in Figure 1 depicts the *OAS* and *PAS* sensors and a gas calibration unit. The gas calibration module is used for generating gas mixtures with ammonia concentrations between 0-100 ppm by mixing gas streams from two cylinders, one containing pure N₂ and the other 100 ppm of NH₃ buffered in N₂ (with a supplier guaranteed precision of $\pm 2\%$). Both cylinders had a stated purity of 99.995%. PC controlled flow controllers regulated the flow rates in each gas stream. The same PC was also used for controlling both sensors and for data acquisition and signal processing. The gas stream was divided into two parts, and directed to the optical absorption (*OA*) and photoacoustic (*PA*) cell, respectively.

2.1. Optical Absorption Spectroscopic sensor

The *OAS* sensor was described in detail in Ref. 15. Here we summarize those physical properties that are important with respect to its comparison with a *PAS* sensor. The main components of the *OAS* sensor are a fiber-coupled, 1.53 μm *DFB* diode laser (NLK1554STB from NEL), with a cw output power of 15 mW, the *OA* cell and a dual beam, auto-balanced

InGaAs photoreceiver (Nirvana 2017 from New Focus Inc.). The *OA* cell is a compact, multi-pass, astigmatically compensated Herriott cell with a total volume of 0.27 liter and an effective optical path-length of 36m, heated to a temperature of 40 °C. Gas was pumped through it at a pressure of 100 Torr using a two-stage diaphragm pump with a flow rate of 2.5 liter/min. The diode laser current was scanned at a rate of 20 Hz with a saw-tooth ramp function over a wavenumber range of 0.3 cm⁻¹, which allowed scanning of the selected ammonia absorption line at 6528.89 cm⁻¹ (1531.65 nm) with a full width at half maximum (*FWHM*) of 0.03 cm⁻¹ and line strength of 1.24x10⁻²¹ cm/molecule⁸. The fiber coupled laser light was directed to a 70/30(%) fiber beam coupler. The larger portion of laser power was transmitted into the *OA* cell, while the beam in the other fiber arm was used as the reference beam for the auto-balancing photoreceiver. The data acquisition and processing software was LabView 5.0, run on a 500 MHz laptop PC. For every single concentration measurement five hundred wavelength scans were averaged. The averaged signal was processed by fitting a Voigt profile to the absorption line and a fifth orders polynomial to the background. The time needed for determining each single ammonia concentration, including data collection, averaging, and signal processing, was ~30 seconds.

2.2. Photoacoustic Spectroscopic gas sensor

In the *PAS* sensor, a temperature stabilized 5 mW fiber pigtailed *DFB* diode laser with the same wavelength as for the *OAS* sensor was used. The laser light output from the fiber was collimated and sent to the *PA* cell. The cell is acoustically optimized, operating with an available continuous gas flow rate of 0.5 liter/min at atmospheric pressure. The *PA* cell (with a volume of ~ 50 cm³) was made of stainless steel. It has a central resonator (of 40 mm length and a 4 mm diameter), where the actual photoacoustic signal generation occurs, and buffer chambers, which are designed for acoustic noise reduction. This *PA* cell was described in

details in Ref. 16. The diode laser wavelength was modulated by combining a constant drive current with a sinusoidally modulated current from a function generator. The modulation frequency was set to coincide with the acoustic resonance of the cell at ~ 4 kHz. At the maximum resonance frequency, the PA cell has its highest efficiency to convert absorbed laser radiation into acoustic energy. This efficiency can be characterized by a cell constant (C), which is the amplitude of the acoustic standing wave generated by unit laser power impinging on a gas sample having unit optical absorption coefficient¹⁷. For an acoustically optimized longitudinal PA cell, as used in these experiments, the cell constant is given by a value of $\sim 2000 \frac{\text{Pa}}{\text{cm}^{-1}\text{W}}$ ^{10,17}. The generated acoustic pressure fluctuation is converted into electrical signal by an electret microphone. This signal is amplified by a microphone pre-amplifier and processed with a lock-in amplifier (SR830, Stanford Research). The lock-in amplifier time constant was set to 10 s. Due to the vector nature of the *PA* signal, both of its real and the imaginary part were measured simultaneously. From the output of the lock-in amplifier, voltages proportional to these signals were fed into the analog-to-digital (*AD*) input of the *PC* data acquisition card. The diode laser wavelength was not scanned, as in the case of *OAS* detection, but after being optimized, kept constant (see section 2.5.).

2.3. Comparison of the physical properties of the PAS and the OAS sensors

The relevant physical properties of the two gas sensors are compared in the first part of Table 1. It can be seen that almost all parameters differ significantly.

The volume of the *OA* cell was three times larger than the volume of the *PA* cell. The *PA* cell volume comes from buffer chambers (49.5 cm^3), and the central resonator (0.5 cm^3). Minimizing the volume of a cell for gas detection purposes has several potential advantages, such as reduction of the size of the entire system, reduction of sample gas consumption, and also faster system response to sudden concentration variations (at least at a fixed gas flow rate).

However, the possibility of size reduction is limited. For the *OA* cell, the main limitation originates from the fact that the light paths in a multi-pass cell cannot overlap due to optical interference effects¹⁸. A *PA* cell volume reduction is limited by acoustic effects¹⁷.

The other significant difference between the two cells is the optical pathlength. In the *OAS* sensor, the measured quantity is the absorbance that is linearly proportional to the pathlength. The longer the pathlength the more intense the *OA* signal. On the other hand, the *PAS* sensor directly measures the optical absorption coefficient (see the definition of the cell constant above), i.e. the *PA* signal is independent of the pathlength (unless a multi-path configuration is used¹⁹). One consequence is the low tolerance of the *OA* cell to laser beam alignment. For the present *OA* cell, 182 reflections of the laser beam within the cell are needed to achieve the long optical pathlength, and thus the alignment of the IR input beam to the cell is critical. The *PA* signal has a much higher tolerance to optical alignment. The material and the operational temperature of the cells are also different. These properties influence the measurements via adsorption-desorption effects.

Both systems were operated at the same NH_3 absorption line (i.e. 1531.65 nm), however the available single frequency *DFB* diode laser powers were different. The laser power used in the *OAS* sensor was three times higher than the diode laser power applied to *PAS* sensor. Since the signal generated by the laser absorption is linearly proportional to the incoming laser power for both systems, this must be taken into account when comparing the sensor performances.

The gas flow rate inside the *PA* cell has a maximum limiting value of ~1 liter/min. Between 0 – 1 liter/min the noise of the *PAS* system is independent of the flow rate, but at this limit an increase in the noise is observed due to the fact that the flow becomes turbulent. For *OAS* detection there is no such limit, and hence the flow rate can be increased by means of a pump capable of a larger flow rate¹⁸.

The operational pressures of the systems were different too. The *OAS* sensor operated at relatively low pressure (100 Torr), which had the advantage of minimizing interference effects from other gas components as well as the possibility of wavelength tuning the diode laser over an absorption line at constant laser temperature by changing the laser current. The *PAS* sensor operated at atmospheric pressure. Pressure dependence was studied in a recent publication for a diode laser based water vapor *PAS* sensor²¹. In the work presented here the pressure was not optimized for the *PAS* system.

2.4. Comparison of the systems from the aspect of background

The backgrounds - defined as the signal measured when the cells are filled with a non-absorbing (e.g. N₂) gas - were found to have significantly different characteristics for the two sensors. In the second part of Table 1 the most important characteristics of the backgrounds are summarized. In the *OAS* system background was mainly introduced by etalon effects. These effects are wavelength dependent and vary with time. The auto-balanced photoreceiver can suppress those etalon effects, which originate from the diode laser and the fiber. However, it cannot compensate etalon effects, generated within the multi-pass cell, and the effect caused by the different spectral response of the two detectors built into the auto-balanced photoreceiver. Therefore, a special software treatment, described in Ref. 15 and based on a 5th order polynomial fitting, was used to reduce these effects. For *PAS* detection the background signal originates from light absorption at the cell windows and walls. Minimization of the background signal requires a straightforward alignment of the *PA* cell, which makes the background signal stable in time and independent of wavelength. On the other hand, the background level depends on the modulation method, especially on the amplitude of the modulation. Therefore the modulation dependence of the background signal as well as the optimum modulation amplitude was determined as follows.

First, the *PA* cell was filled with 100 ppm NH_3 buffered in N_2 . Various combinations of a steady and a modulated part of the diode laser current were selected to maintain a constant maximum current (40 mA). For each current combination, the diode laser temperature was optimized to obtain a maximum *PA* signal. The same combination of diode laser currents and temperature was also used for measuring the photoacoustic background signal by filling the *PA* cell with pure nitrogen. The results of these measurements are depicted in Fig. 2., which also shows the ratio of the signal to the background as a function of the modulation current amplitude. There were two criteria for selecting the optimum current modulation depth, a high photoacoustic signal and a stable background. Measurements of the background were carried out for several days first at maximum signal (right hand side of Fig. 2.) and then at maximum signal-to-background ratio in order to make such a modulation selection. In the former case, the background signal showed long-term drifts, which exceeded fluctuations caused by acoustic and electric noises. No such drift was observed when the system was operated at the maximum signal-to-background configuration. Therefore, for the remainder of the measurements, the current setting (34 mA dc and 6 mA modulated) that yielded the maximum signal-to-background ratio was selected.

It is worth noting that for low power (few mWs) diode laser based *PAS* sensors, the background signals exhibit low levels (after alignment). Its fluctuations are primarily due to acoustic and electric noises, which are independent of the background signal level¹⁰. On the other hand, for high power (several hundred mW) diode laser based *PAS* sensors, background signal fluctuations (attributed e.g. to laser power fluctuations or beam pointing instability) were found to limit the performance of the sensor²². In this case the level of background fluctuations depends on the level of the background signal. Although in the present case the laser power is relatively low, the background drift was shown to influence the concentration measurements, at least at high modulation amplitude.

Since the background signal was stable in time, it was necessary to measure it only once and subtract it from the actual *PA* signal. However, as the origin of the background signal is different from the useful signal, this subtraction has to be performed in a phase-correct way, i.e. taking into account the vector nature of both signals.

2.5. Comparison of the operating modes of the PAS and OAS sensors.

The modes of operations of the two sensors are summarized in the third part of Table 1. In the case of the *OAS* sensor noise suppression was performed by averaging 500 wavelength scans. The number of scans was optimized to sensor performance, such as the minimum detectable concentration (*MDC*) and response time and was limited by long term sensor instabilities mainly due to temperature fluctuations. The *FWHM* of the pressure narrowed NH_3 line was 10 times smaller than the total wavelength scanning window, and therefore the measured spectrum was ideal for line profile fitting. The fitted Voigt profile provided an absolute method for determination of the concentration based on the knowledge of laser power, optical pathlength, optical absorption coefficient of the laser line and the sensitivity of the detector¹⁵.

For the *PAS* sensor, wavelength modulation was used with an optimized diode laser current and temperature configuration (see section 2.4 and Fig. 2.). The *PA* signal was detected with a lock-in amplifier with the averaging time set to 10 s. Unlike the *OAS* system, the *PAS* system has to be calibrated. In the present case the *OAS* sensor was used as a reference.

3. Results and Conclusions

The performances of the systems could be compared from several aspects (such as size, reliability, ease of operation and maintenance, *MDC*, response time and cost). In this work the *MDC* and the response time (listed in the last part of Table 1) were compared. These

performance characteristics are determined by the physical properties, background effects and modes of operation.

The calibration of the *PAS* sensor was performed by using predetermined NH_3 concentrations in a randomly selected sequence. After setting a gas mixing ratio, the sensors were purged with this mixture for ~ one hour before a measurement, in order to ensure that both sensors reached steady state response values. The *PA* signal as function of the ammonia concentration measured by the *OAS* sensor is shown in Fig. 3. The value of the *PA* signal is plotted prior to amplification (i.e. the lock-in amplifier signal divided by the amplification of the microphone pre-amplifier). The ammonia concentration is calculated from the *OA* signal directly¹⁵. The measurement points in Fig. 3. could be fitted with a calibration line using a correlation coefficient (*R*) of $R^2=0.9999$, indicating excellent agreement between *OA* and *PA* signals. This agreement is remarkable if one considers the difference in the sensor systems. Neither adsorption-desorption processes, nor the difference in the way the absorbed laser power is measured by the two sensors perturb the signals. Actually, this calibration was found to be more reliable than calibrating the *PAS* sensor to the concentration calculated from flow rates set by the flow controllers.

The *MDC* for both systems were calculated in terms of three times the standard deviation of the measured background signals (IUPAC regulations). In this way, a *MDC* value of 0.6 ppm for the *PAS* system and 0.7 ppm for the *OAS* system were derived, which are lower than the 1 ppm value reported in Ref. 16.

The *PA* cell constant can be calculated from the calibration curve in Fig 3, which has a slope of 0.28 $\mu V/ppm$. The microphone sensitivity as specified by its supplier is 50 mV/Pa. The optical absorption coefficient for the absorption line is equal to $5.8 \times 10^{-7} \text{ cm}^{-1}/ppm^8$. From these data (and the laser power of 5 mW) a cell constant of 1930 Pa/cm⁻¹/W can be calculated, which is in good agreement with the previously published value¹⁶.

The systems were also tested in measurements, which simulated real-world measurements of dynamically varying ammonia concentrations. Random ammonia concentrations were generated as follows. The flow rate of the nitrogen was kept constant, while the flow of the 100 ppm ammonia + nitrogen mixture was changed every 30 minutes by supplying randomly generated voltages to its flow controller. A segment of the measurements is shown in Fig. 4. From these measurements the time constant was found to be ~1 minute and ~3 minutes for the *OAS* and *PAS* sensors, respectively. This time constant is approximately 10 times longer in both cases than the time needed to purge the cells with a new concentration, which can be defined as the cell volume divided by the flow rate. This relatively slow response can be attributed to the adsorption-desorption effects of the ammonia molecules on the walls of the *OA* and *PA* cells. Despite the differences between the cells, the response times are in the same range. These measurements demonstrate the applicability of the systems to concentration measurements in real-world applications.

In summary, cross calibration of a photoacoustic and an optical absorption spectroscopic systems, both based on fiber-coupled telecommunication *DFB* diode lasers, proved that both sensors can operate with sub-ppm level sensitivity. Both analyzer systems are capable of automatic, unattended operation. However, the *PAS* system is less sensitive to optical alignment and in some applications offers the advantage of small size, ease of operation and minimum maintenance.

Acknowledgements

The research at Rice University was funded by NASA, the Texas Advanced Technology program and the Welch Foundation. Partial funding of the work by the Hungarian National Research and Development Program (3/061/2001) and by the OTKA foundation (D 37791) is gratefully acknowledged.

References:

1. G. Ramis, L. Yi and G. Busca, *Catalysis Today* **28**, 373 (1996).
2. I. Linnerud, P. Kaspersen and T. Jaeger, *Appl. Phys. B* **67**, 297 (1998).
3. R.A. Rooth, A.J.L. Verhage and L.W. Wouters, *Appl. Opt.* **29**, 3643 (1990).
4. L. R. Narasimhan, W. Goodman and C. K. N. Patel,
www.pnas.org/cgi/doi/10.1073/pnas.071057598
5. M. Fehér and P.A. Martin, *Spectrochimica Acta* **A51**, 1579 (1995).
6. Á. Mohácsi, M. Szakáll, Z. Bozóki, G. Szabó and Z. Bor, *Laser Physics*. **10**, 378 (2000).
7. L. S. Rothman, *HITRAN2000 Database* <http://cfa-www.harvard.edu/HITRAN>.
8. M. E. Webber, D. S. Baer, R. K. Hanson, *Applied Optics*. **40**, 2031 (2001).
9. G. Liang, H. Liu, A. H. Kung A. Mohácsi, A. Miklós and P. Hess, *J. Phys. Chem. A* **104**, 10179 (2000).
10. Z. Bozóki, J. Sneider, Z. Gingl, Á. Mohácsi, M. Szakáll, Z. Bor and G. Szabó, *Measurement Science and Technology* **10**, 999 (1999).
11. M. W. Sigrist, *Air Monitoring by Spectroscopic Techniques* (Wiley: New York, 1994.)
12. M. Fehér, P.A. Martin, A. Rohrbacher, A. Soliva and J.P. Maier, *Appl. Opt.* **32**, 2028 (1993).
13. M. Fehér, Y. Jiang, J.P. Maier and A. Miklós, *Appl. Opt.* **33**, 1655 (1994).
14. S. Schäfer, M. Mashni, J. Sneider, A. Miklós, P. Hess, V. Ebert, K.-U. Pleban and H. Pitz, *Appl. Phys. B* **66**, 511 (1998).
15. R. Claps, F. V. Englich, D. P. Leleux, D. Richter, F. K. Tittel and R. F. Curl, *Appl. Optics* **40**, 4376 (2001).
16. A. Miklós, P. Hess, Á. Mohácsi, J. Sneider, S. Kamm, and S. Schäfer, *Photoacoustic and Photothermal Phenomena: 10th International Conference*, edited by F. Scudieri and M. Bertolotti, (American Institute of Physics, Woodbury, NY, 1999) p.126.

17. A. Miklós, P. Hess and Z. Bozóki, *Rev. Sci. Instrum.* **72**, 1937 (2001).
18. J. B. McManus, P. L. Kebedian, and M. S. Zahniser, *Appl. Optics* **34**, 3336 (1995).
19. M. Nagele and M.W. Sigrist, *Applied Physics. B.* **70**, 895 (2000).
20. A. Schmohl, A. Miklós and P. Hess, *Appl Optics* **40**, 2571 (2001).
21. M. Szakáll, Z. Bozóki, M. Kraemer, N. Spelten, O. Moehler and U. Schurath, *Environ. Sci. Technol.* **35**, 4881 (2001).
22. L. Krämer, Z. Bozóki and R. Niessner, *Analytical Sciences* **17**, 563 (2001).

Table caption

Table 1. Comparison of the *OAS* and the *PAS* sensors.

Figure captions

Fig. 1. Experimental set-up.

Fig. 2. *PA* signal (open triangles) and background signal (open squares) as a function of laser modulation amplitude. Also shown is the signal-to-background ratio (closed squares).

Fig. 3. *PA* signal as a function of ammonia concentration measured by the *OAS* sensor.

Fig. 4. Randomly varying NH_3 concentration set by flow controllers (solid line) and measured by the *PAS* sensor (open circles) and by the *OAS* sensor (closed circles).

		OAS system	PAS system	Comments	
Physical Properties	Cell	Volume	270 cm ³	50 cm ³	OAS: limited by optical effects PAS: limited by acoustic effects
		Optical pathlength	36 m	9 cm	OAS: signal is proportional to absorbance. PAS: signal is proportional to optical absorption coefficient.
		Material	Glass	Stainless steel	The material and the temperature of the cell affect adsorption-desorption processes
		Temperature stabilization	Heated to 40 °C	None	
	Laser power	15 mW	5 mW	Signal is linearly proportional to laser power for both systems	
	Flow rate	2.5 liter/min.	0.5 liter/min.	OAS: can be increased up to 10 liter/min ¹⁸ . PAS: limited by flow generated noise	
	Operational pressure	100 Torr	atmospheric pressure	OAS: optimized for line-profile fitting PAS: not optimized	
Background (BG)	Origin	Etalon effects	Absorption by cell windows and walls	OAS: wavelength dependent PAS: independent of wavelength	
	Time dependence	Varies in time	Stable in time	OAS: measured simultaneously PAS: measured only during calibration	
	Experimental treatment	Balanced detection	Optimization of modulation depth	OAS: limited by etalon effects within the cell PAS: operated at maximum signal to BG ratio	
	Mathematical treatment	Polynomial fit	Subtraction from signal	OAS: using the off-absorption part of the recorded spectra PAS: with correct phase	
Mode of operation	Noise reduction methods	Averaging of wavelength scans (500 scans)	Wavelength modulation Lock-in detection (integration time: 10s)	OAS: Absorption line-width determines the wavelength scanning range. PAS: Modulation amplitude is optimized for maximum signal-to-background ratio.	
	Determination of concentration	Via fitted parameters	Calibrated to OAS	OAS: absolute PAS: linear calibration curve was found	
Performances	Minimum detectable concentration, (MDC)	0.7 ppm	0.6 ppm	OAS and PAS are limited by etalon effects and by acoustic and electric noise, respectively.	
	Response time	1 minute	3 minutes	~ 10 times the purging time (volume divided by flow rate) for OAS and PAS	

Table 1. Z. Bozóki et. al.

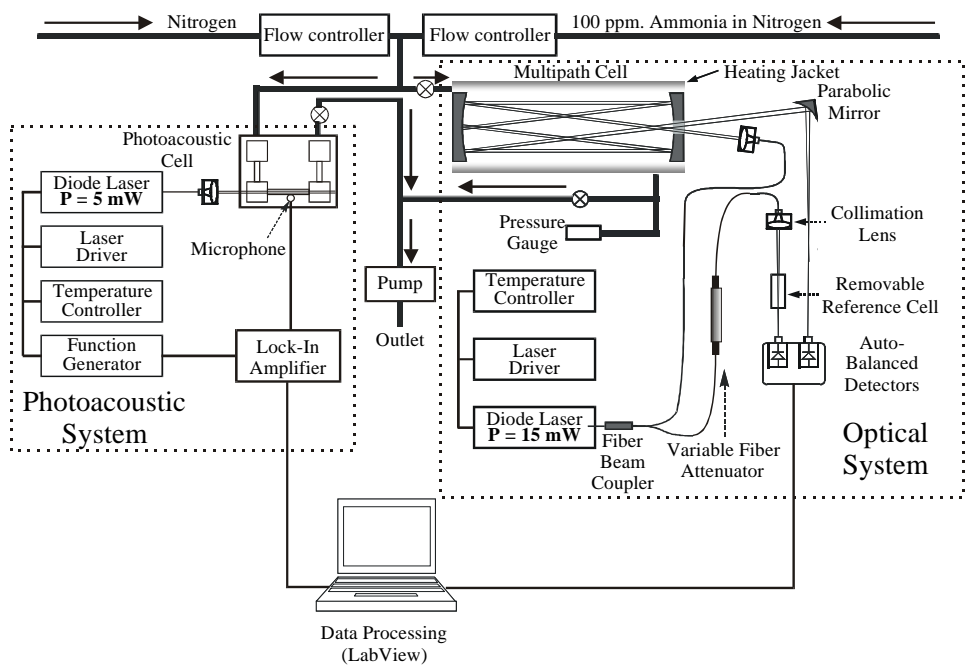


Fig. 1. Z. Bozóki et. al.

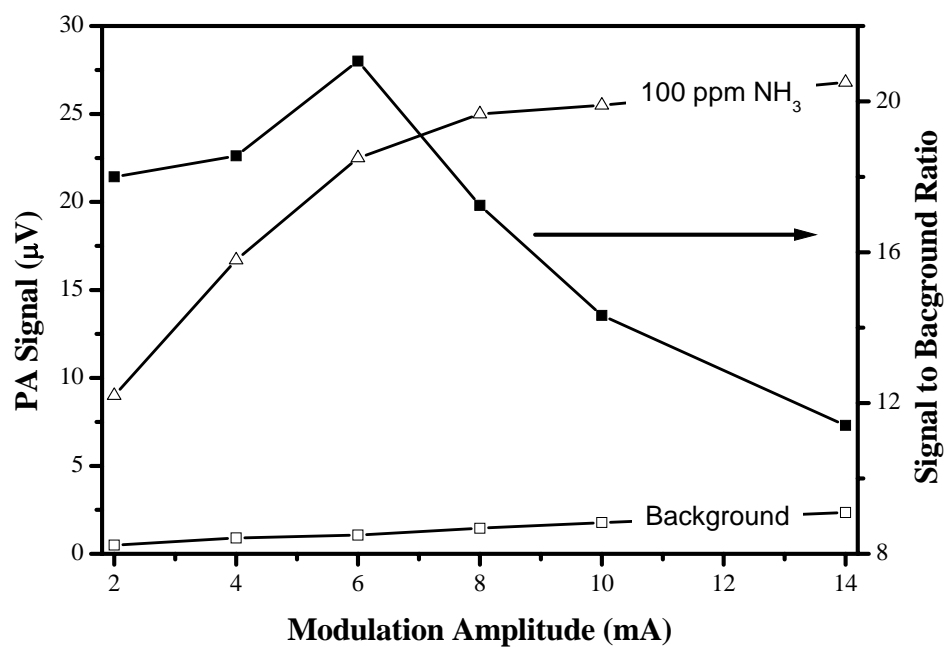


Fig. 2. Z. Bozóki et. al.

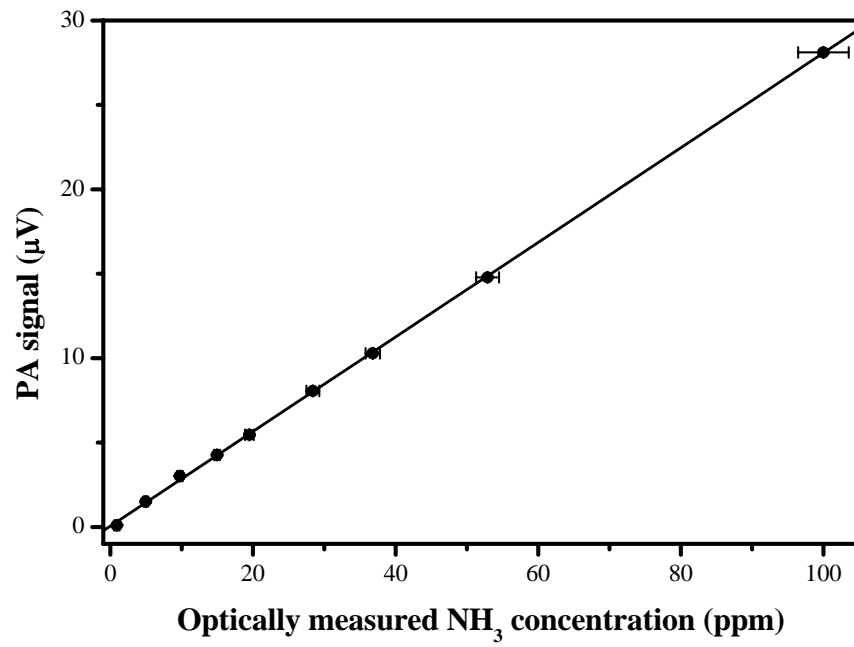


Fig. 3. Z. Bozóki et. al.

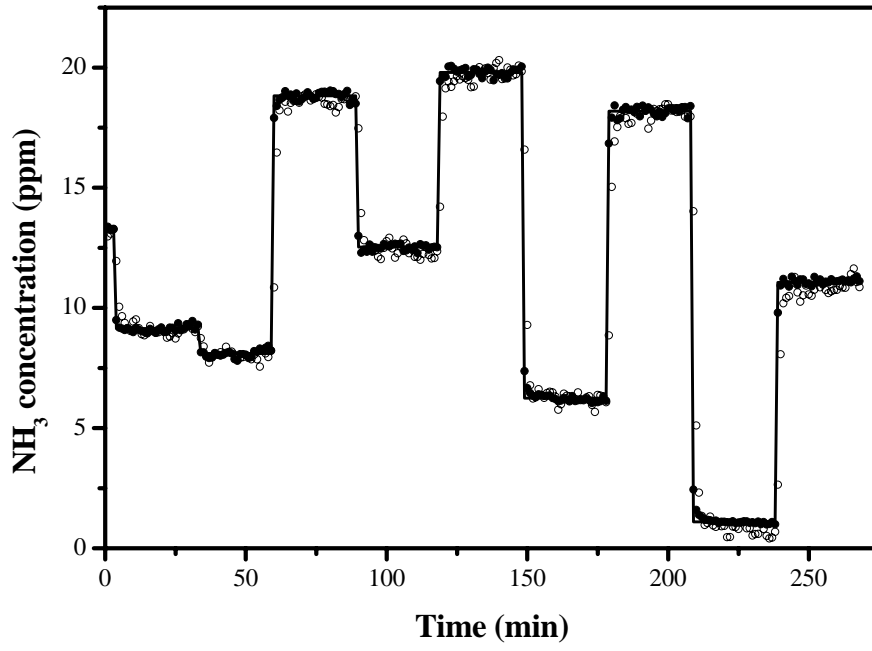


Fig. 4. Z. Bozóki et. al.